Hubble Tension: Constraining the Hubble parameter using time-delay gravitational lensing experiments and comparison with other methods

Lauren Jade Thomas

December 19, 2023

Abstract

Hubble tension is one of the biggest mysteries facing modern observational cosmologists' in recent years. For nearly 100 years, researchers and theorists alike have been trying to calculate the rate at which the universe is expanding. Our current understanding of the universe is dependent on the ΛCDM model; however, when this model is used in conjunction with early universe probes, a statistically significant 4σ to 6σ discrepancy appears when compared to multiple, model-independent, late universe probes that utilise measured distances and observed redshifts. In this review, I primarily focus on one such late universe technique; strong gravitational lensing. I start by outlining the underlying theory of the phenomenon with a brief mathematical framework, including an introduction to how galaxy lenses are modelled and how these systems are used to calculate the Hubble constant. I provide a brief overview of both early and late universe probes and the most current results determined by these methods, focusing on recent strong gravitational lensing surveys and their model designs. I look at how we could reconcile this tension, whether it can be explained by invoking systematic uncertainties or whether refinements in lens modelling approaches, future data collection and processing techniques (or a combination of all three) will be sufficient for eliminating this tension with strong gravitational lensing alone or if there is a call to re-evaluate our current cosmological model.

Contents

Chapter 1

Introduction

1.1 Background

The Hubble constant is the rate at which the universe expands at any given time. The Hubble constant is derived from Hubble's law, the observation in physical cosmology that galaxies are moving away from the Earth at speeds that are proportional to their distance. It is one of the most compelling pieces of evidence that supports Big Bang Cosmology, which underpins our present-day understanding of the universe.

The Hubble constant, H_0, can be calculated from astronomical data in multiple ways. In this review, I focus on using strong gravitational lensing systems. Refsdal (1964) concluded that per the laws of General Relativity, the path of light from a background star would be deflected by the gravitational field of a foreground star. This phenomenon has been well tested, and we have even observed the gravitational lensing by entire galaxies (and galaxy clusters) since the discovery of the first gravitationally lensed quasar by Walsh et al. (1980). Since then, this technique has been used extensively to constrain the value of the Hubble constant.

In this project, I examine how this technique has been used to calculate values of the Hubble constant. Explore why different lensing systems and early and late universe methods do not always return the same value; after all, the Hubble constant should be constant.

1.2 Objectives

1. Survey and summarily describe the underlying theory behind the various approaches for calculating the Hubble constant.
2. Explain how strong gravitational lensing can be and is used to calculate the Hubble constant to a high degree of precision and how this is achieved.
3. Explore recent experimental work that uses time-delay cosmography to calculate the Hubble constant, evaluating the underlying methodology's strengths and weaknesses and how different techniques lead to differing values for H_0.
4. Suggest how the discrepancy between early and late values of H_0 could be resolved in future, examining sources of error and potential gaps in our understanding.

1.3 Scope of work

This project focuses on gravitational time delay lensing, how this technique is used in the field of time delay cosmography to calculate the universe's rate of expansion, and how these values conflict with those derived using direct and indirect methods. The underlying theory of other methods will not be discussed in great detail, but an overview will be provided where necessary for comparison purposes.

1.4 Search methodology

- A combination of SAO/NASA astrophysics data system, Smithsonian Astrophysical Observatory (2022), arxiv.org, and google scholar primarily searching for "Gravitational lensing" AND "Hubble tension" (or AND "Hubble constant") and references therein.
- Reviewing the publications from large research collaborations websites (notably *TDCOSMO* (2022) & *H0LiCOW* (2022) and papers referenced therein).

- Evaluated each paper using the PROMPT criteria, The Open University (2014), to evaluate the suitability of papers selected to shortlist for the report's central themes.
- The papers and books included in the resources provided as part of the SXP390 module materials included in the gravitational lensing topic: primarily a citation search from the 33rd Saas-Fee Advanced Course - Gravitational lensing: Strong, Weak & Micro, Kochanek et al. (2004).

Chapter 2

Gravitational lensing theory

2.1 General Relativity to Gravitational lensing

The main takeaway of the theory of General Relativity is that the presence of any mass alters the geometry of spacetime; it is because of this fundamental property of spacetime that gravitational lensing occurs. Photons emitted from astronomical sources are assumed to be radiated uniformly in all directions; when we think of light as a particle, we expect the light to travel in a straight line between source and observer. Light would travel in straight lines if spacetime were entirely flat; it is not at local scales.

This review focuses specifically on strong gravitational lensing; strong lensing occurs when a lens has a mass density in projection above a particular critical density (as defined by the individual system) which leads to both the multiplication and magnification of the source, as seen by the observer. In simple terms, it can be understood as an optical mapping between the (true) source plane and an observed image plane. However, gravitational lenses differ from conventional optical lenses because they have no single focal point but rather lines of theoretically infinite magnification known as critical lines. When these critical lines are transferred back to the source plane, they are called caustics. The location of these lines is both dependent on the relative distance between the source and lens plane and the matter distribution within the lens itself. The position of the source with respect to its relevant caustic (as governed by its distance from the lens) determines the arrangement of the (often multiple, discrete) images and their magnifications.

2.1.1 Deflection angle

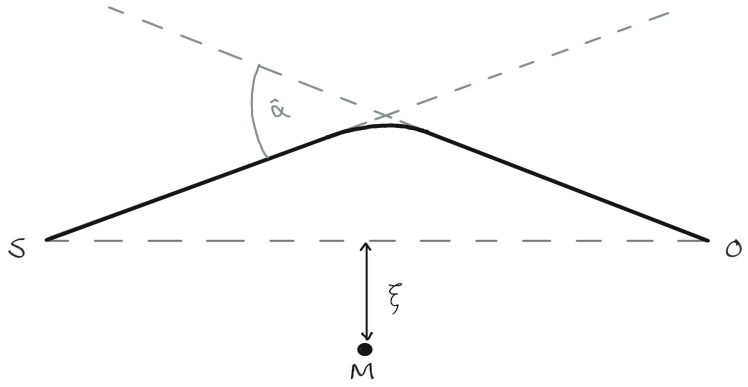

Figure 2.1: Simple point mass lens diagram, where S is the position of the source, O is the position of the observer, M is the mass of the lens, and ξ is the impact parameter—created by author.

Suppose we examine a point mass gravitational lens (Figure 2.1) and the equations that govern General relativity (for a complete derivation, see Carroll (2004)) we can derive an equation that tells us the gravitational deflection angle $\hat{\alpha}$ in terms of the mass of the lens, M, the Gravitational constant, G = $6.6743 \times 10^{-11}\ m^3\ kg^{-1}\ s^{-2}$ and impact parameter ξ.

$$\hat{\alpha} = \frac{4GM}{\xi}$$

2.1.2 Thin screen approximation

Most of the deflection by a gravitational lens occurs near the lens, within $z \sim \xi$. This allows us to treat all deflection as if it occurs in the lens plane. We can use the thin screen approximation because the distance between the lens and source and the lens and observer is far more significant than the lens size.

2.1.3 The Lens equation

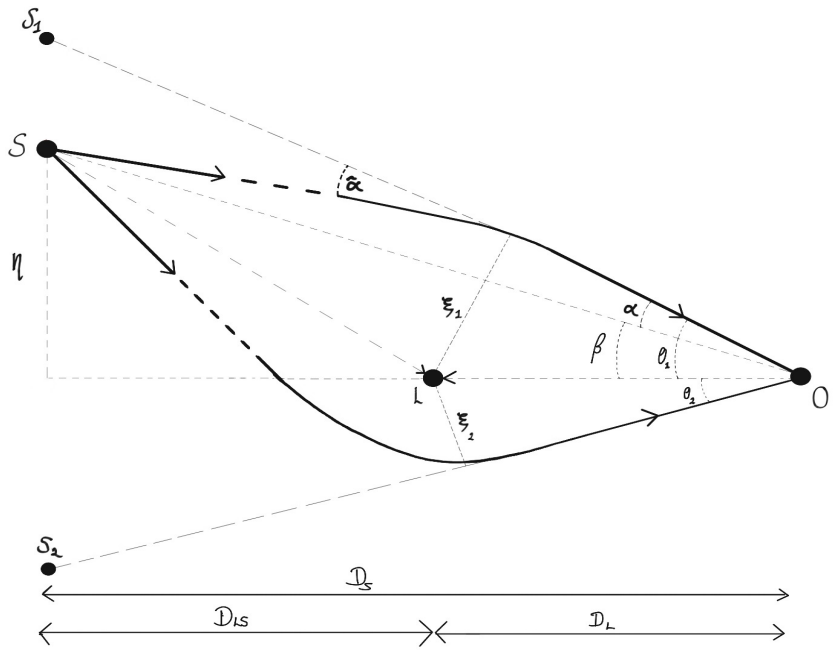

Figure 2.2: A Strong gravitational lensing system wherein S, L and O are the source, lens and observer, respectively. $\hat{\alpha}$ is the deflection angle, α is the scaled deflection angle, η is the 2D position of the source in the source plane, β is the angular position of the source (if there were no lens), and θ is the observed angular position. ξ_1 and ξ_2 are the impact parameters for the top and bottom paths, respectively. Created by author.

If we apply the thin screen approximation to the strong gravitational lensing system outlined in Figure 2.2, the small-angle approximation can be used; as well as the thin lens equation:

$$\alpha(\theta) = \frac{D_{LS}}{D_S}\,\hat{\alpha}(D_S\theta) \qquad \eta = D_S\,\beta$$
$$\beta = \theta - \alpha(\theta) \qquad \xi = D_L\,\theta$$

In our understanding of the universe, the ΛCDM model specifies that the universe is flat. These equations hold true as long as space has zero curvature; if space has any degree of curvature, then $D_{LS} \neq D_S - D_L$. This means that gravitational lensing is one of the few model-independent tests on whether this assumption is accurate.

The extent of a mass's lensing effect can be determined mathematically; in the case of a point mass, it would have a perfectly circular lens with a radius equal to the lens's Einstein radius, θ_E.

$$\theta_E = \sqrt{\frac{4GM}{c^2}\frac{D_{LS}}{D_S D_L}}$$

When $\beta > \theta_E$, the source is weakly lensed, which results in one weakly distorted image. When $\beta < \theta_E$, the source is strongly lensed, and multiple images are formed. If $\beta = \theta_E$ then an Einstein ring is formed. As in Figure 2.2, in strong gravitational lensing systems, there can be multiple solutions/values for β and, thus, multiple discrete images. For strong lensing to occur; the projected surface density, Σ, must also exceed the critical density given by

$$\Sigma_{CR} = \frac{c^2}{4\pi G}\ \frac{D_S}{D_L D_{LS}}$$

2.1.4 Magnification

Gravitational lensing preserves surface brightness but alters the apparent solid angle of the source due to magnification. In the general case, magnification calculated using the lens equation is

$$\mu = \left| \ det\left(\frac{\partial\beta}{\partial\theta}\right) \ \right|^{-1} \equiv \left| \ det\left(\frac{\partial\beta_i}{\partial\theta_j}\right) \ \right|^{-1}$$

If the lens is circularly symmetric, this reduces to

$$\mu = \frac{\theta}{\beta}\frac{\partial\theta}{\partial\beta}$$

In the example of a point mass:

Images occur at

$$\theta_{\pm} = \frac{1}{2}\,(\beta \pm \sqrt{\beta + 4\theta_E^2}), \quad u = \beta\theta_E^{-1}$$

Magnification is

$$\mu_{\pm} = \left[1 - \left(\frac{\theta_E}{\theta_{\pm}}\right)^4\right]^{-1} = \frac{u^2+2}{2u\sqrt{u^2+4}} + \frac{1}{2}$$

If the value is positive, the source is magnified. If it is negative, it can go either way; it is dependent on the system.

The total magnification is

$$\mu = |\mu+| + |\mu_-| = \frac{u^2+2}{u\sqrt{u^2+4}}$$

When the source is on the Einstein ring: $\beta = \theta_E, u = 1$

2.1.5 Shapiro Time Delay

Due to the presence of the mass-created lens, light rays take different paths toward the observer and therefore take different amounts of time to reach the observer. The time delay between each image (as measured by the total redshift of each image) underpins how time-delay cosmography can experimentally determine the Hubble constant. Time-delay measurements have the additional benefit of being completely independent of the cosmic distance ladder.

Time delays were first outlined by Shapiro (1964) and are defined by the equation:

$$\Delta t = -\int \Phi \; ds$$

The total time delay is the sum of the path lengths from deflection and the gravitational time delay.

$$\begin{aligned} t(\vec{\theta}) &= \frac{(1+z_d)}{c}\frac{D_L D_S}{D_{LS}}\left[\frac{1}{2}(\vec{\theta}-\vec{\beta})^2 - \psi(\vec{\theta})\right] \\ &= t_{geom} + t_{grav} \end{aligned}$$

2.2 Galaxy Lensing and Constraining H_0

2.2.1 Single Isothermic Sphere

Galaxy lenses require that we accurately account for the distribution of matter within the lens. The simplest way to do this is by assuming a model that treats all the galactic mass like particles in an ideal gas. Therefore we can use the ideal gas equation and related phenomena to define the system. This approach allows lenses created by a galaxy (or a cluster of galaxies) to be treated like a point-mass lens. As such, we expect a minimum of two images to be formed. The magnification can be substantial, especially for sources directly aligned with the lens; when this happens, an Einstein ring is formed.

2.2.2 Mass Determination

The time-delay depends on the total matter distribution within a lensing galaxy, both baryonic and dark. A simple estimate of the total mass can be obtained if we assume a perfectly spherical lens because the critical mean density will equal the mean surface density contained within the Einstein radius.

In practice, one needs to take into account the mass-sheet transformation (MST); the mass distribution, $k(\theta)$, isotropically scales with λ (term representing the MST). (Falco et al. (1985))

$$\kappa_\lambda(\theta) = \lambda\kappa(\theta) + (1 - \lambda)$$

The MST scales everything from the source position to H_0 and time-delay distance equally, and it is impossible to determine from optical images alone - this is called mass-sheet degeneracy (MSD) (Schneider and Sluse (2013)). However, including spectroscopy or stellar kinematics data can break this degeneracy; it is also worth considering that the MST also has external components; for example, the distribution of matter in the line-of-sight (LOS) should also be accounted for - Rusu et al. (2017).

Whilst the time-delay distance is most sensitive to the value of H_0; it is still weakly dependent on the values of the matter density, σ_m, dark energy density, σ_{de}, the dark energy equation of state, w, and the curvature parameter, σ_k. (Suyu and Halkola (2010) & Linder (2011)).

2.2.3 H_0 Determination

As outlined above, the total time-delay has two components; geometric and gravitational. The geometric element can be found from the angular distances D_L, D_S and D_{LS} and the redshift, z. The gravitational component $\phi(\theta, \beta)$ is dependent on the mass distribution (convergence) $\kappa(\theta)$ since $\kappa(\theta) = \frac{1}{2}\nabla^2\psi(\theta)$ where $\psi(\theta)$ is the lensing potential of the galaxy. This is why lens modelling is crucial because, without it, there is no way to account for the MST's scaling of H_0. Time-delay can be measured, so time-delay distance $D_{\Delta t}$ can be calculated. The Hubble constant is inversely proportional to the scales of the universe, ergo $H_0 \propto D_{\Delta t}^{-1}$. The degeneracy needs to be broken to calculate a value for λ, so an accurate inference of H_0 can be made.

Chapter 3

Constraining H_0 experimentally

Methods for determining the Hubble constant from experimental data fall into two distinct groups; indirect and direct. The currently accepted values of the cosmological parameters (Table 3.1) are derived from indirect methods. These methods utilise the analysis of the anisotropies in Cosmic Microwave Background Radiation (CMBR). These are called early universe measurements in the literature since they look at matter distribution 'shortly' after the big bang. Direct methods, or late universe measurements, pertain to calculations made from astronomical phenomena researchers have directly observed.

3.1 Early Universe Probes

3.1.1 WMAP and Planck

Efforts to calculate the value of the Hubble constant in the early universe utilise the anisotropies in the CMBR. Using the data gathered by both the Wilkinson Microwave Anisotropy Probe (WMAP) and the European Space Agency's (ESA) Planck probe (also known as the Planck Collaboration), detailed images of the CMBR were created.

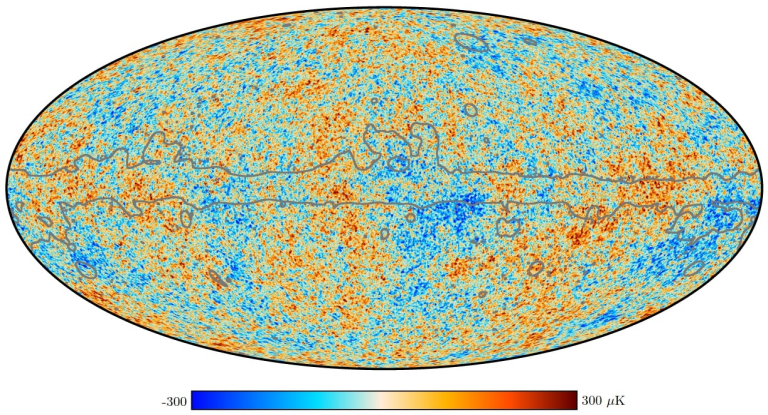

Figure 3.1: The 2018 Planck map shows the temperature anisotropies found in the CMB. The bright yellow and red spots represent areas of increased temperature, which directly correspond to matter distribution in the early (and present-day) universe. (European Space Agency (2018)).

Parameter:	**Symbol:**	**Final Value:**
Scalar spectral index	n_s	0.9665 ± 0.0038
Age of the universe	t_0	$13.787 \pm 0.020 \ \times 10^9$ years
Optical depth due to reionization	τ	0.0561 ± 0.0071
Physical baryon density	$\Omega_b h^2$	0.02242 ± 0.00014
Physical dark matter density	$\Omega_c h^2$	0.11933 ± 0.0041
Curvature fluctuation amplitude[1]	Δ^2_R	$2.441^{+0.088}_{-0.092} \times 10^{-9}$
Hubble constant ($km\ s^{-1} Mpc^{-1}$)	H_0	67.66 ± 0.42
Dark energy density	Ω_Λ	0.6889 ± 0.0056
Matter density	Ω_M	0.3111 ± 0.0056

Table 3.1: The six independent parameters of the ΛCDM model of the universe and the calculated values of the Hubble constant, Dark Energy density and overall matter density from Aghanim et al. (2020). [1] - From Jarosik et al. (2011)

3.1.2 Baryonic Acoustic Oscillations (BAOs) and BOSS

The anisotropies visible in the CMBR are directly related to the position of matter in the present-day universe. The physics of propagation of baryonic matter before recombination is well understood, which allows cosmologists to calculate the size of the sound horizon at recombination. The distribution of matter in the CMBR and the present-day universe is the same; as the universe has aged, it has expanded at the rate defined by the Hubble constant equally in all directions. By comparing the position of galaxy clusters (for example) to the anisotropies in the CMBR, researchers can calculate the expansion rate without relying on data from other techniques, Eisenstein et al. (2005).

The latest result derived using this technique is from Alam et al. (2021), the team behind the extended Baryonic Oscillations Spectroscopic Survey (eBOSS) found using data from the Sloan Digital Sky Survey's 16th data release (SDSS DR16) that $H_0 = 68.20 \pm 0.81\ km\ s^{-1} Mpc^{-1}$ at a 68% confidence level (CL) when assuming the standard ΛCDM model.

3.1.3 Dark Energy Survey

The Dark Energy Survey (DES) employed the 'inverse distance ladder' method to calibrate the absolute magnitude of 329 Type Ia Supernovae (SNIa), using absolute distance measurements derived from BAOs. MacAulay et al. (2019) found that when used in combination, the value of $H_0 = 67.8 \pm 1.3\ km\ s^{-1} Mpc^{-1}$ (68% CL) when taking into account statistical and systematic uncertainties. This value agrees with values calculated from the CMBR and negates the previous tension.

3.2 Late Universe Probes

3.2.1 Cosmic Distance Ladder

Direct measurements that allow the calculation H_0 are many and varied. One of the most common techniques relies on the cosmic distance ladder, which allows astronomers to calculate astronomical distances through various methods. The Hubble constant can be calculated when the distance to an object with known composition and redshift is examined. The use of trigonometric parallaxes is limited to objects within approximately 1000 parsecs of Earth, so standard candles are used. A standard candle is an object of known luminosity; by comparing the known luminosity to the observed brightness, the distance can be modelled using an inverse-square law.

This technique has been used to calculate various values of H_0; the Supernovae H_0 for the Equation of State (SH0ES) team recently presented their findings from a 15-year effort to create a robustly calibrated distance ladder. By using the distances to hundreds of Cepheid variable stars and SNIa to calibrate their distance ladder they generated an estimate of $H_0 = 74.03 \pm 1.42\ km\ s^{-1} Mpc^{-1}$ (Riess et al. (2019)).

The distance ladder is reliant on calibration; the Carnegie-Chicago Hubble Program (CCHP) used stars at the Tip of the Red Giant Branch (TRGB) to calibrate their distance ladder and found $H_0 = 69.8 \pm 0.6$ (statistical) $\pm$ 1.6 (systematic) $km\ s^{-1} Mpc^{-1}$. These results from Freedman (2021) significantly reduce the tension between early and late universe measurements but rely on local measurements and appear to diverge at larger distances. The most recent paper from SH0ES, Riess et al. (2022), uses both Cepheid and TRGB calibration of SNIa and found $H_0 = 72.53 \pm 0.99\ km\ s^{-1}\ Mpc^{-1}$, so whilst accuracy appears to be increasing, we cannot wholly disregard the need to improve either our methods or understanding.

3.2.2 Strong Gravitational Lensing

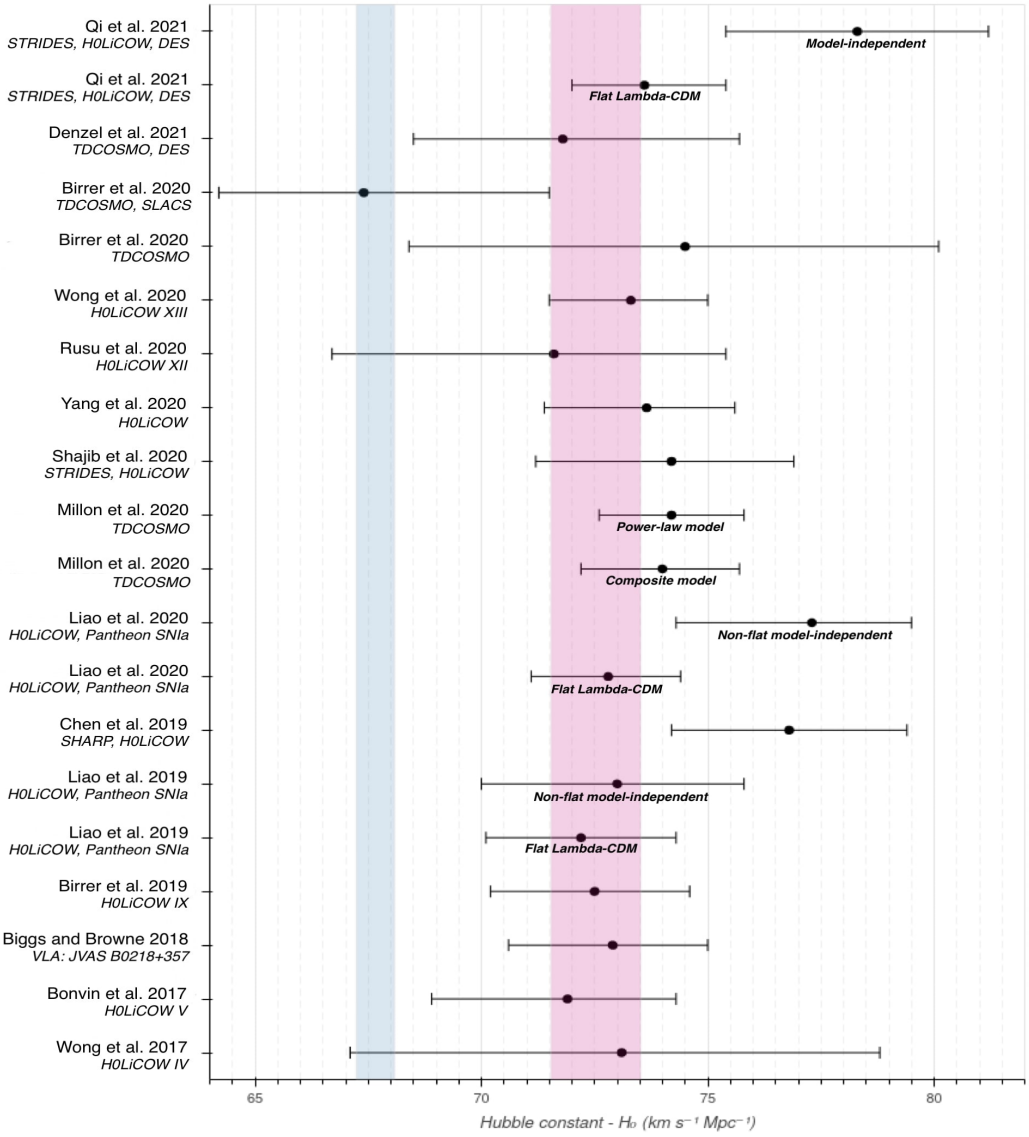

Figure 3.2: A whisker plot of strong gravitational lensing derived values of the Hubble constant from 2017 to 2022. Different analyses from the same paper are listed separately. The blue band represents the values from Planck, Aghanim et al. (2020) and the pink band the most recent results from SH0ES, Riess et al. (2022) - Created by author.

Unfortunately, these values exist in significant tension with early universe measurements. The main challenge is to create an accurate mass distribution model which can be used to make an accurate inference of the time-delay distance.

Lens mass distribution models are parameterised mass models where observational data define the parameters. However, it is possible to create a model that perfectly fits the observed characteristics of a lensing system, leading to a completely wrong inference of the time-delay distance (Bonvin et al. (2017)). One needs to take special care when attempting to break the Mass-Sheet degeneracy; the use of a simple power-law density model can lead to a bias on H_0 of between 20-50% (Xu et al. (2016)). This can, however, be mitigated with the use of stellar kinematics data, Sonnenfeld (2018) found that the combination of the power-law density profile and stellar kinematics data for double-lensed systems can be used to calculate H_0 with a 3% accuracy.

It is worth highlighting that Birrer et al. (2019) modelled the doubly imaged quasar SDSS 1206+4332 using a composite model for the deflector galaxy, taking into account both baryonic and dark matter and the deflector galaxy's velocity dispersion. Combined with the characteristics of the quasar host galaxy, nearby perturbing galaxies and the line of sight structure, $H_0 = 68.8^{+5.4}_{-5.1}\ km\ s^{-1}Mpc^{-1}$ with an overall precision from a single lens of 7.2%. However, when combined with three previous H0LiCOW lenses, taking into account the statistical likelihood of these systems, they found $H_0 = 72.5^{+2.1}_{-2.3}\ km\ s^{-1}Mpc^{-1}$. Whilst the uncertainties are significant, this value does appear to be in relative agreement with early universe measurements.

It, therefore, becomes clear that values calculated from strong gravitational lenses are only ever as precise as their lensing models. Numerous components must be considered, as discussed above and in Chapter 2; it can be challenging to constrain all the possible compounding variables with the data available. Therefore researchers have started to use external datasets to help 'fill in the gaps' as outlined below.

3.2.3 Combining Multiple Datasets

The measurements from multiple lensing systems are often combined to form a composite sample, and lenses are also frequently reanalysed. For example, Yang et al. (2020) reanalysed four of H0LiCOW's (H0 Lenses in COsmograil's Wellspring) lenses, for which they had calculated time-delay distances and distances inferred from stellar kinematics data and found $H_0 = 73.65^{+1.95}_{-2.26}\ km\ s^{-1}Mpc^{-1}$. TDCOSMO I, (Millon et al. (2020)) combined six lenses from the H0LiCOW sample and one lens from STRIDES (STRong lensing insights into Dark Energy Survey) and when assuming a power-law lens models, calculated $H_0 = 74.2 \pm 1.6\ km\ s^{-1}Mpc^{-1}$.

TDCOSMO IV (Birrer et al. (2020)) reanalysed the TDCOSMO dataset, eschewing previous mass models and choosing to constrain models using only stellar kinematics data and found $H_0 = 74.5^{+5.6}_{-6.1}\ km\ s^{-1}Mpc^{-1}$. Combined with imaging and spectroscopy data from 33 strong lenses in the Sloan Lens ACS (SLACS) dataset and joint hierarchical analysis, they calculated $H_0 = 67.4^{+4.1}_{-3.2}\ km\ s^{-1}Mpc^{-1}$.

The findings from this analysis do not statistically invalidate the mass models used in the previous H0LiCOW analyses; it does highlight the need for a thorough understanding of the mass profiles of elliptical deflector galaxies. This finding is an excellent example of the potential of using external datasets to create a generalised statistical model. However, the errors are significant, partially due to the uncertainties in the stellar kinematics data. In part due to the use of spherical jeans modelling (model of the stellar velocity dispersion) as well as the 10% scatter in the values of λ_{int} used to break the MSD of the TDCOSMO lenses and partially due to the assumption that the lenses are from the same parent population and therefore share significant characteristics.

In the future, they expect that with additional time-delay and non-time-delay lenses from SLACS and the Strong Lensing Legacy Survey, precision will increase to 1.2%, thereby resolving the Hubble tension at 3σ to 5σ without making assumptions about the radial mass profiles of deflector galaxies, Birrer and Treu (2021).

The values presented thus far all rely on the current understanding of the universe, the flat ΛCDM model. Some attempts to separate the calculation of H_0 from the late behaviour of the ΛCDM model have been undertaken, Liao

et al. (2019) use four strongly lensed quasar systems from H0LiCOW and data from the Pantheon SNIa compilation, using a gaussian process regression to create an estimate of $H_0 = 72.2 \pm 2.1\ kms^{-1}Mpc^{-1}$ in a flat universe, ($H_0 = 73.0^{+2.8}_{-3.0}\ km\ s^{-1}Mpc^{-1}$ when allowing for a cosmic curvature density $\sigma_k = [-0.2, 0.2]$), later updated in Liao et al. (2020) with the use of six lenses from H0LiCOW to $H_0 = 72.8^{+2.1}_{-1.7}\ kms^{-1}Mpc^{-1}$ and $H_0 = 77.3^{+2.2}_{-3.0}\ km\ s^{-1}Mpc^{-1}$ in a similarly non-flat universe.

Chapter 4

Reconciling Early and Late Measurements

How can we reconcile these results with each other, and is it possible to resolve this tension with our current understanding?

The measurement of CMB anisotropies has resulted in incredibly precise values of the six required independent cosmological parameters of the standard model of Big Bang cosmology. (In this case, Occam's razor requires a minimum of six independent parameters to create an acceptable fit for current observations). If we assume that the current model is correct, the calculated value of the Hubble constant from this data set ought to be the actual value. As I have shown so far, an overwhelming body of evidence from direct observations contradicts this value.

4.1 Systematic Errors

The most cynical explanation is to focus on these methods' often significant uncertainties; however, this feels very reductionist. Any single systematic error would need to affect every calculated value equally. A singular systematic error is improbable, if not impossible, given the size of the discrepancy between calculated values from indirect and direct methods and the sheer number of independent direct methods yielding similar values. Each method is independent of the others and individually affected by different systematic uncertainties, yet all agree. The likelihood of completely independent systematic errors affecting each experiment in all these measurements, in

the same way, feels slim to none. However, the systematic errors in CMB measurements cannot explain this tension either.

There is a formal way to combine unknown systematic errors between multiple experiments using the BACCUS (BAyesian Conservative Constraints and Unknown Systematics) framework. This method was first introduced by Bernal and Peacock (2018) to allow for combining multiple direct methods, all of which are independent of each other. Their average included direct measurements using the distance ladder, BAOs, time-delay cosmography, cosmic clocks (the use of differential ages of old elliptical galaxies that estimate of the inverse of the Hubble parameter $H(z)^{-1}$) and light curve analysis from SNIa. They found a total average of $H_0 = 72.7 \pm 1.2(2.9)\ km\ s^{-1}Mpc^{-1}$ at a confidence level of 68(95)%, which is still in significant tension with the value calculated by Planck.

4.2 Future Research

The question becomes; why is there such a significant difference? It can't be denied that there is room for improvement in lens modelling methods; there is an obvious need for more constraints on these mass models. At the time of writing, the first images from the James Web Space Telescope/Near InfraRed Camera (JWST/NIRCam) have recently become available. Caminha et al. (2022) [preprint: July 2022] have just unveiled the first strong gravitational lens mass model created using this new data. They generated a mass model for the lens SMACS J0723.3-7327 from pre-JWST data (19 multiple images from 6 background sources, 4 of which have associated spectroscopic data) and a refined model from JWST data (an additional 27 images and no additional spectroscopic data). The uncertainties in the JWST model are already 33% lower without the inclusion of spectroscopic data. With the inclusion of the spectroscopic data included in Mahler et al. (2022) [preprint: July 2022], the mass model of SMACS J0723.3-7327 will undoubtedly become even more precise. Only time will tell if this increase in precision modelling will resolve the Hubble tension or if our current cosmological model needs to be adapted.

So far, our attempts to tackle the problem of the Hubble tension all rely on one thing; data. With surveys from the JWST and the Rubin Observatory Legacy Survey of Space and Time (LSST) Dark Energy Science Collaboration (DESC), we are anxiously awaiting an explosion in the amount of data

available. This, however, poses its problems. Converting these data points into a workable model for each lens is time-consuming and laborious.

I find the approach suggested by Sonnenfeld (2021) and Sonnenfeld (2022) to be the most hopeful for breaking the H_0 lens model degeneracy with observational data alone. However, he determined that the sample size required to create a parameterised model for a population of galaxies would require the computer modelling of well over 100 lenses supplemented by data from non-lensing galaxies - a population of solely strongly lensing galaxies is inherently biased - to determine the true properties of a galaxy population. Creating 100 models from real observational data has been unachievable thus far, even if we had data on 100 lenses.

It is a genuine possibility that we will be able to collect enough data to break the degeneracy in the near future, so perhaps the most pressing question is how we are going to process it and create robust models for each system? I think the answer will lie in applying machine learning to the task. Neural networks have seen a recent explosion in both popularity and research and development in recent years. Neural networks are computer systems designed to mimic the biological structure of the human brain; they are engineered primarily for pattern recognition. We are starting to see various fields adopt this approach in novel ways.

Won Park et al. (2021) have pioneered a Bayesian Neural Network (BNN) for large-scale lens modelling, explicitly aiming to infer the value of the Hubble constant precisely. Their network has generated an individual lens model for each of their 200 simulated lenses in less than 10 minutes each. It was able to determine the value of the Hubble constant (as decided by the researchers in creating the training set, the computer did not know this value) to within 0.5 $km\ s^{-1}Mpc^{-1}$ with no detectable bias; this corresponds to an error of 0.7%.

A general rule with these networks is that the more data there is in the training dataset, the more accurate they become, so if this approach is applied to future datasets, it should certainly be possible to calculate the actual value of H_0 to the same degree of accuracy.

4.3 The Case For New Physics

It is hard to say whether we need to re-evaluate our current cosmological model based on the information we have; however, it would be naive to assume that the flat ΛCDM model is perfect in every way and that there isn't room for future discoveries. The Hubble tension has been a significant conundrum for many years and the focus of many researchers' careers. Numerous solutions have been suggested that attempt to reduce or remove the tension between measurements - for a comprehensive review of possible solutions, I recommend Di Valentino et al. (2021).

There is a genuine possibility that we could eliminate the uncertainties in lensing-derived values using JWST and LSST data, possibly in conjunction with machine learning, allowing us to calculate a value of H_0 with as much precision as Planck. I am convinced that with more data from more strong lenses, combined with the use of a robustly trained BNN, we will be able to determine once and for all if the value of H_0 has changed over time and whether it varies in the local universe to any degree. Either it will resolve the tension or won't; either way, we will have an answer.

Chapter 5

Conclusions

5.1 Summary

In this review, I have described the underlying theory of how we get from the laws of General Relativity to using strong gravitational lenses to calculate the Hubble constant. I have outlined how this technique has been used in recent research and the various considerations needed to generate increasingly precise and accurate lens models. The field is an auspicious one; I believe that with a larger sample of lenses combined to create a generalised statistics-based model for a given parent population of galaxies, we should be able to calculate an accurate value of the Hubble constant using (direct observational) lensing data alone. This should allow us to determine whether the tension between the early and late universe measurements is a product of flawed methodology or flawed understanding.

5.2 Achievement of Project Objectives

1. Survey and summarily describe the underlying theory behind the various approaches for calculating the Hubble constant. - **Chapter 2**

2. Explain how strong gravitational lensing can be and is used to calculate the Hubble constant to a high degree of precision and how this is achieved. - **Chapter 3**

3. Explore recent experimental work that uses time-delay cosmography to calculate the Hubble constant, evaluating the underlying methodology's strengths and weaknesses and how different techniques lead to differing values for H_0. - **Chapter 3**

4. Suggest how the discrepancy between early and late values of H_0 could be resolved in future, examining sources of error and potential gaps in our understanding. - **Chapter 4**

5.3 Author's Note

This paper represents the literature review dissertation for my BSc (Hons) Natural Sciences (Astronomy and Planetary Sciences) issued by The Open University (Milton Keynes, United Kingdom) in October of 2022. My brief was to conduct a literature review related to my previous study in a current area of astronomy research presented in less than 5000 words; this work is designed to be accessible to any undergraduate or postgraduate student of General Relativity. I am making this work available via arXiv in the hopes that other students and non-specialists find it a helpful introduction to this exciting area of research. I have no intention of submitting this to a journal, only to leave it here for posterity. If you wish to contact me for any reason, please email me at arxiv@ljaytee.me.

Bibliography

Aghanim, N. et al. (2020). 'Planck 2018 results: VI. Cosmological parameters'. *Astronomy and Astrophysics* 641, A6. Available at: https://doi.org/10.1051/0004-6361/201833910.

Alam, S. et al. (2021). 'THE COMPLETED SDSS-IV EXTENDED BARYON OSCILLATION SPECTROSCOPIC SURVEY:COSMOLOGICAL IMPLICATIONS FROM TWO DECADES OF SPECTROSCOPIC SURVEYS AT THEAPACHE POINT OBSERVATORY'. *Physical Review D* 8.103. Available at: https://doi.org/10.1103/PhysRevD.103.083533.

Bernal, J.L. and J.A. Peacock (2018). 'Conservative cosmology: combining data with allowance for unknown systematics'. *Journal of Cosmology and Astroparticle Physics* 2018 (07), p. 002. Available at: https://doi.org/10.1088/1475-7516/2018/07/002.

Birrer, S and T Treu (2021). 'TDCOSMO - V. Strategies for precise and accurate measurements of the Hubble constant with strong lensing'. *Astronomy & Astrophysics* 649, A61. Available at: https://doi.org/10.1051/0004-6361/202039179.

Birrer, S. et al. (2019). 'H0LiCOW - IX. Cosmographic analysis of the doubly imaged quasar SDSS 1206+4332 and a new measurement of the Hubble constant'. *Monthly Notices of the Royal Astronomical Society* 484.4, pp. 4726–4753. Available at: https://doi.org/10.1093/mnras/stz200.

Birrer, S. et al. (2020). 'TDCOSMO - IV. Hierarchical time-delay cosmography – joint inference of the Hubble constant and galaxy density profiles'. *Astronomy & Astrophysics* 643, A165. Available at: https://doi.org/10.1051/0004-6361/202038861.

Bonvin, V. et al. (2017). 'H0LiCOW - V. New COSMOGRAIL time delays of HE 0435-1223: H0 to 3.8 per cent precision from strong lensing in a flat ΛCDM model'. *Monthly Notices of the Royal Astronomical Society*

465.4, pp. 4914–4930. Available at: https://doi.org/10.1093/mnras/stw3006.

Caminha, G.B. et al. (2022). 'First JWST observations of a gravitational lens Mass model of new multiple images with near-infrared observations of SMACS J0723.37327'. Available at: https://doi.org/10.48550/arXiv.2207.07567.

Carroll, S.M. (2004). *Spacetime and Geometry: An Introduction to General Relativity*. 8. Addison Wesley. ISBN: 0805387323.

Di Valentino, E. et al. (2021). 'Classical and Quantum Gravity In the realm of the Hubble tension-a review of solutions'. *Classical and Quantum Gravity* 38 (153001). Available at: https://doi.org/10.1088/1361-6382/ac086d.

Eisenstein, D.J. et al. (2005). 'Detection of the Baryon Acoustic Peak in the Large-Scale Correlation Function of SDSS Luminous Red Galaxies'. *The Astrophysical Journal* 633.2, pp. 560–574. Available at: https://doi.org/10.1086/466512/XML.

European Space Agency (2018). *Picture Gallery - Planck - Cosmos*. URL: https://www.cosmos.esa.int/web/planck/picture-gallery (visited on 07/20/2022).

Falco, E.E., M.V. Gorenstein, and I.I. Shapiro (1985). 'On model-dependent bounds on H 0 from gravitational images : application to Q 0957+561 A, B.' *The Astrophysical Journal* 289, pp. L1–L4. Available at: https://doi.org/10.1086/184422.

Freedman, W. (2021). 'Measurements of the Hubble Constant: Tensions in Perspective*'. *The Astrophysical Journal* 919.1, p. 16. Available at: https://doi.org/10.3847/1538-4357/AC0E95.

H0LiCOW (2022). URL: https://shsuyu.github.io/H0LiCOW/site/ (visited on 07/06/2022).

Jarosik, N. et al. (2011). 'SEVEN-YEAR WILKINSON MICROWAVE ANISOTROPY PROBE (WMAP*) OBSERVATIONS: SKY MAPS, SYSTEMATIC ERRORS, AND BASIC RESULTS'. *The Astrophysical Journal* 192.2, p. 17. Available at: https://doi.org/10.1088/0067-0049/192/2/14.

Kochanek, C.S., P. Schneider, and J. Wambsgnass (2004). *Proceedings of the 33rd Saas-Fee Advanced Course: Gravitational lensing: Strong, Weak & Micro*. Ed. by G. Meylan, P. Jetzer, and P. North. Heidelberg: Springer-Verlag Berlin. ISBN: 978-3-540-30310-7. Available at: https://doi.org/10.1007/978-3-540-30310-7.

Liao, K. et al. (2019). 'A Model-independent Determination of the Hubble Constant from Lensed Quasars and Supernovae Using Gaussian Process Regression'. *The Astrophysical Journal Letters* 886.1, p. L23. Available at: https://doi.org/10.3847/2041-8213/AB5308.

Liao, K. et al. (2020). 'Determining Model-independent H0 and Consistency Tests'. *The Astrophysical Journal Letters* 895.2, p. L29. Available at: https://doi.org/10.3847/2041-8213/AB8DBB.

Linder, E.V. (2011). 'Lensing Time Delays and Cosmological Complementarity'. *Physical Review D - Particles, Fields, Gravitation and Cosmology* 84.12. Available at: https://doi.org/10.1103/PhysRevD.84.123529.

MacAulay, E. et al. (2019). 'First cosmological results using Type Ia supernovae from the Dark Energy Survey: Measurement of the Hubble constant'. *Monthly Notices of the Royal Astronomical Society* 486.2, pp. 2184–2196. Available at: https://doi.org/10.1093/mnras/stz978.

Mahler, G. et al. (2022). 'Precision modeling of JWST's first cluster lens SMACS J0723.37327 *'. Available at: https://doi.org/10.48550/arXiv.2207.07101.

Millon, M. et al. (2020). 'TDCOSMO - I. An exploration of systematic uncertainties in the inference of H0 from time-delay cosmography'. *Astronomy Astrophysics* 639, A101. Available at: https://doi.org/10.1051/0004-6361/201937351.

Refsdal, S. (1964). 'THE GRAVITATIONAL LENS EFFECT*'. *Monthly Notices of the Royal Astronomical Society* 128.4, pp. 295–306. Available at: https://doi.org/10.1093/mnras/128.4.295.

Riess, A. et al. (2019). 'Large Magellanic Cloud Cepheid Standards Provide a 1% Foundation for the Determination of the Hubble Constant and Stronger Evidence for Physics beyond ΛCDM'. *The Astrophysical Journal* 876.1, p. 85. Available at: https://doi.org/10.3847/1538-4357/AB1422.

Riess, A. et al. (2022). 'A Comprehensive Measurement of the Local Value of the Hubble Constant with 1 km s1 Mpc1 Uncertainty from the Hubble Space Telescope and the SH0ES Team'. *The Astrophysical Journal Letters* 934.1, p. L7. Available at: https://doi.org/10.3847/2041-8213/AC5C5B.

Rusu, C.E. et al. (2017). 'H0LiCOW – III. Quantifying the effect of mass along the line of sight to the gravitational lens HE 04351223 through weighted galaxy counts'. *Monthly Notices of the Royal Astronomical So-*

ciety 467.4, pp. 4220–4242. Available at: https://doi.org/10.1093/MNRAS/STX285.

Schneider, P and D Sluse (2013). 'Mass-sheet degeneracy, power-law models and external convergence: Impact on the determination of the Hubble constant from gravitational lensing'. *Astronomy & Astrophysics* 559, A37. Available at: https://doi.org/10.1051/0004-6361/201321882.

Shapiro, I.I. (1964). 'Fourth Test of General Relativity'. *Physics Review Letters* 13 (26), pp. 789–791. Available at: https://doi.org/10.1103/PhysRevLett.13.789.

Smithsonian Astrophysical Observatory (2022). *The SAO/NASA Astrophysics Data System*. URL: https://ui.adsabs.harvard.edu/classic-form.

Sonnenfeld, A. (2018). 'On the choice of lens density profile in time delay cosmography'. *Monthly Notices of the Royal Astronomical Society* 474 (4), pp. 4648–4659. Available at: https://doi.org/10.1093/MNRAS/STX3105.

Sonnenfeld, A. (2021). 'Astrophysics Statistical strong lensing II. Cosmology and galaxy structure with time-delay lenses'. *Astronomy & Astrophysics* 656, p. 153. Available at: https://doi.org/10.1051/0004-6361/202142062.

Sonnenfeld, A. (2022). 'Statistical strong lensing - III. Inferences with complete samples of lenses'. *Astronomy & Astrophysics* 659, A132. Available at: https://doi.org/10.1051/0004-6361/202142301.

Suyu, S.H. and A. Halkola (2010). 'The halos of satellite galaxies: the companion of the massive elliptical lens SL2SJ085440121'. *Astronomy & Astrophysics* 524.4, A94. Available at: https://doi.org/10.1051/0004-6361/201015481.

TDCOSMO (2022). URL: http://www.tdcosmo.org/index.html (visited on 05/27/2022).

The Open University (2014). *Advanced evaluation using PROMPT*. URL: https://www.open.ac.uk/libraryservices/documents/advanced-evaluation-using-prompt.pdf.

Walsh, D., R.F. Carswell, and R.J. Weymann (1980). '0957 + 561 A, B: twin quasistellar objects or gravitational lens?' *Nature* 279.5712, pp. 381–384. Available at: https://doi.org/10.1038/279381a0.

Won Park, J. et al. (2021). 'Large-scale Gravitational Lens Modeling with Bayesian Neural Networks for Accurate and Precise Inference of the Hubble Constant'. *The Astrophysical Journal* 910 (1), p. 39. Available at: https://doi.org/10.3847/1538-4357/ABDFC4.

Xu, D. et al. (2016). 'Lens galaxies in the Illustris simulation: power-law models and the bias of the Hubble constant from time delays'. *Monthly Notices of the Royal Astronomical Society* 456 (1), pp. 739–755. Available at: https://doi.org/10.1093/MNRAS/STV2708.

Yang, T., S. Birrer, and B. Hu (2020). 'The first simultaneous measurement of Hubble constant and post-Newtonian parameter from time-delay strong lensing'. *Monthly Notices of the Royal Astronomical Society: Letters* 497.1, pp. L56–L61. Available at: https://doi.org/10.1093/MNRASL/SLAA107.